Feedback Control of the Safety Factor Profile in DIII-D Advanced Tokamak Discharges

J.R. Ferron 1), V. Basiuk 2), T.A. Casper 3) E.J. Doyle 4), Q. Gao 5) P. Gohil 1), C.M. Greenfield 1), F. Imbeaux 2), J. Lohr 1), T.C. Luce 1), M.A. Makowski 3), D. Mazon 2), M. Murakami 6), Y. Ou 7), J.-M. Park 8), C.C. Petty 1), P.A. Politzer 1), T.L. Rhodes 4), M. Schneider 2), E. Schuster 7), M.A. Van Zeeland 9), M.R. Wade 1), and A. Wang 5)

1) General Atomics, P.O. Box 85608, San Diego, California 92186-5608, USA
2) Association Euratom-CEA, CEA-Cadarache, France
3) Lawrence Livermore National Laboratory, Livermore, California, USA
4) University of California-Los Angeles, Los Angeles, California, USA.
5) Southwest Institute of Physics, Chengdu, China.
6) Oak Ridge National Laboratory, Oak Ridge, Tennessee, USA
7) Lehigh University, Bethlehem, Pennsylvania, USA
8) National Fusion Research Center, Dae Jeon, Korea
9) Oak Ridge Institute for Science Education, Oak Ridge, Tennessee, USA

e-mail contact of main author: ferron@fusion.gat.com

Abstract. Active feedback control for regulation of the safety factor (q) profile at the start of the high stored energy phase of an Advanced Tokamak discharge has been demonstrated in the DIII-D tokamak. The time evolution of the on-axis or minimum value of q is controlled during and just following the period of ramp-up of the plasma current using electron heating to modify the rate of relaxation of the current profile. In L-mode and H-mode discharges, feedback control of q is effective with the appropriate choice of either off-axis electron cyclotron heating or neutral beam heating as the actuator. The q profile is calculated in real time from a complete equilibrium reconstruction fitted to external magnetic field and flux measurements and internal poloidal field measurements from the motional Stark effect diagnostic. This is the first use of this accurate calculation method for real time q profile identification and control. Comparisons of experimental measurements and transport code predictions of the time evolution of the current profile are used to validate transport codes for use in testing of real time feedback control algorithms. In some cases, the modeled noninductive current must be located farther from the axis than is predicted by theory in order to obtain agreement between the simulations and the experiment.

1. Introduction

A key feature of an advanced tokamak (*AT*) discharge [1] is safety factor (q) and plasma pressure profiles that are consistent with both magnetohydrodynamic (MHD) stability at high toroidal β and a high fraction of the self-generated bootstrap current ($\beta = 2\mu_0 \langle P \rangle / B^2$, $\langle P \rangle$ is the volume averaged plasma pressure, B is the toroidal magnetic field). Appropriate profiles will enable high fusion gain and noninductive sustainment of 100% of the plasma current for steady-state operation [2]. The approach taken toward establishing an *AT* discharge in the DIII-D tokamak is to create the desired q profile during the plasma current ramp-up and early flattop phases with the aim of maintaining this target profile during the subsequent high β phase using off-axis electron cyclotron current drive (ECCD), on-axis fast wave current drive, bootstrap current and neutral beam current drive (NBCD). We report here results from experiments at DIII-D on feedback controlled formation of the target q profile [3]. The feedback control is implemented using changes in the plasma conductivity to modify the rate of relaxation of the profile of the inductive component of the plasma current. Comparisons of experimental measurements of the time evolution of the current profile and transport code

predictions are used to aid in interpretation of experimental results and to validate transport codes for use in testing of real time feedback control algorithms.

The initial evolution of q on axis, $q(0)$, and the minimum value of q, q_{min}, during and just following the period of ramp-up of the plasma current, has been the focus of the first feedback control experiments in DIII-D. An example [2] of the type of discharge used is shown in Fig. 1. The high β phase begins at 3.4 s [Fig. 1(b)] when approximately 100% of the plasma current is sustained noninductively, as indicated by the zero loop voltage [Fig. 1(d)]. The goal of the feedback is to control $q(0)$ and q_{min} beginning with the relatively high values just after the plasma breakdown [Fig. 1(c)] to reproducibly arrive at the values to be sustained in steady-state, $1.5 < q_{min} < 2.5$ and $q(0) - q_{min} \approx 0.5$, at the beginning of the high β phase. Feedback control is necessary in order to adapt to variations in the current profile created at discharge breakdown and in the density and impurity profiles during the current ramp-up.

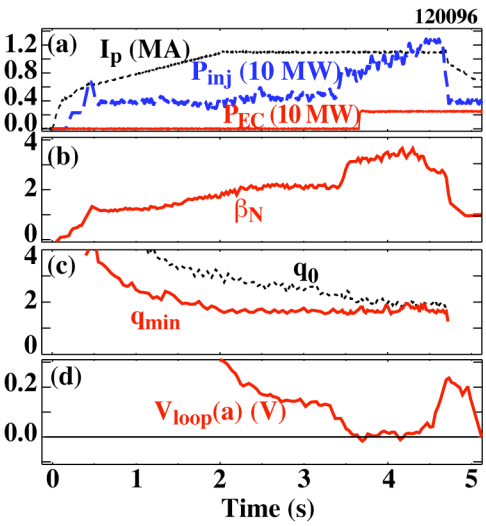

FIG. 1. The time evolution of a DIII-D AT discharge with 100% of the plasma current driven noninductively as indicated by loop voltage near zero during the high β phase. (a) Plasma current (I_p), smoothed neutral beam power (P_{inj}), gyrotron power (P_{EC}), (b) normalized beta ($\beta_N = \beta aB/I_p$ where a is the minor radius, I_p is the plasma current in MA and β is in percent), (c) minimum and on-axis safety factor, (d) loop voltage at the plasma surface.

The primary available control actuator for the current profile evolution during the plasma formation is the conductivity [4,5] (σ) profile. The rate of relaxation of the inductive current profile depends strongly on the conductivity [6]. It is difficult to use noninductive driven current as an actuator during this phase of the discharge because it is calculated [2] to be <40% of the total current, modification of the shape of the neutral-beam-driven and bootstrap current profiles is difficult and the calculated ECCD efficiency (≈0.013 A/W) is low because of the relatively low β and electron temperature T_e. So, because of the strong dependence of σ on T_e, electron heating is used as the actuator for the $q(0)$ and q_{min} evolution [7-9]. At DIII-D, off-axis electron cyclotron heating (ECH) and neutral beam heating have both been used to change the σ profile. This concept of using modifications of the σ profile to modify the time evolution of the profile of the inductively driven current differs from the use of sources of localized current drive for feedback control [3] to maintain a constant current profile in steady state when the inductive component is zero.

2. Open Loop Measurements

Open loop experiments were used to demonstrate the modifications in the q profile evolution that result from changes in T_e. This is illustrated in Fig. 2 where the effect of the value of T_e is compared for the L-mode [Figs. 2(a-d)] and the H-mode [Figs. 2(e-h)]. In the H-mode cases, the L-H transition was induced very early in the discharge, at ≈500 ms. In Cases 1, 2, and 4, ECH resonant at normalized radius $\rho \approx 0.4$ is used to hold T_e at a nearly constant level, while in the other two cases no ECH is applied. In the L-mode cases, the T_e profile, and thus the conductivity profile, is relatively peaked so the strongest effect of increasing T_e is to

reduce the decay rate of $q(0)$. The evolution of q_{min}, located near the mid-radius, is only slightly affected. In the H-mode case, the T_e profile is much broader as a result of the edge-region transport barrier. As a result, the conductivity in the region outside the radius of q_{min} is 2-4 times larger in the H-mode discharges than in the L-mode discharges so that the rate of relaxation of the inductive current in that region is smaller and both q_{min} and $q(0)$ are significantly increased when T_e is raised. An additional result of the broader σ profile is that the q values are higher in the H-mode cases for a longer duration compared to the L-mode discharges for comparable mid-radius values of T_e. So, the choice between L-mode and H-mode is also an effective means to modify the q profile evolution because of the change in the shape of the conductivity profile [8].

3. Real Time Identification of the *q* Profile

To enable closed loop feedback control, the q profile is calculated in real-time from a complete equilibrium reconstruction. Data from 26 internal poloidal field measurements from the motional Stark effect (MSE) diagnostic provide constraints on the reconstructed current profile. The real-time EFIT algorithm [10] is used to find a least squares fit solution to the Grad-Shafranov tokamak

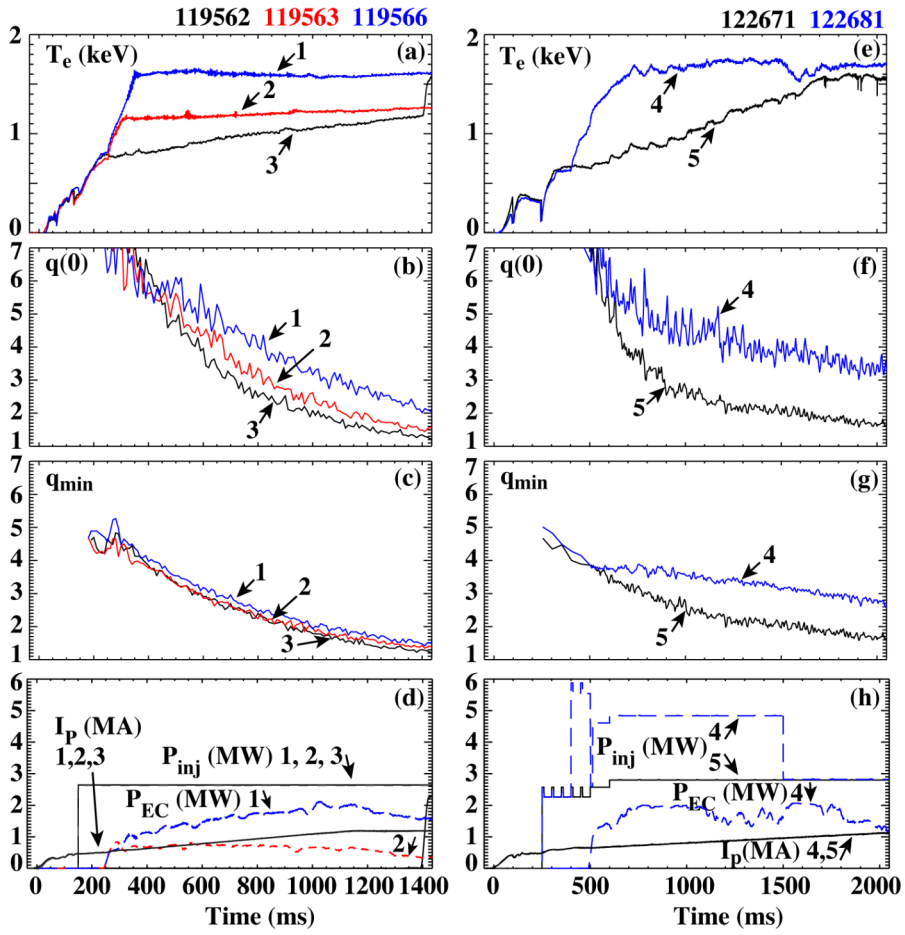

FIG. 2. Time evolution of (a,e) electron temperature at ρ ≈ 0.4, (b,f) on-axis q, (c,g) minimum value of q and (d,h) smoothed neutral beam power P_{inj}, smoothed gyrotron power P_{EC} and total plasma current I_p in discharges with various values of T_e. The discharges in (a-d) are L-mode and the discharges in (d-h) are H-mode. In Cases 1, 2 and 4, T_e is feedback controlled using ECH at ρ ≈ 0.4 while Cases 3 and 5 have no ECH.

equilibrium relation that matches the MSE and external magnetic field and flux measurements. Thus the q profile is calculated from a current profile solution that is consistent with force balance. This is the first use of this type of equilibrium reconstruction for real-time identification and control of the q profile. Improvements that have been made to the equilibrium reconstruction algorithm since the publication of Ref. [10], made possible by faster computers, include correction for the effect of the radial electric field on the MSE measurement [11], spline parameterization of the current profile [12] to allow accurate identification of q profiles with negative central magnetic shear, fitting of the measured poloidal field coil currents (rather than treating the currents as known values) in order to allow for measurement uncertainties, and the possibility to use multiple iterations in an equilibrium reconstruction. Full profiles of q are available in real time at 4 ms intervals if only one iteration is used, but three iterations are commonly used in order to reduce the noise in the q profile reconstruction, in which case the interval is 8 ms. There are only small differences between the values of $q(0)$ and q_{min} obtained in real time for feedback control and the results obtained from off-line calculations with the EFIT [12] code.

4. Closed Loop Feedback Control

Closed loop control of the q evolution has been successfully tested in both L-mode and H-mode using either ECH at $\rho \approx 0.4$ or neutral beam power as the actuator for modification of T_e. Two examples of feedback control of $q(0)$ in L-mode discharges using off-axis ECH are compared in Fig. 3 with a case without ECH. The control here is on $q(0)$ because, as illustrated in Fig. 2, there is little ability to modify q_{min} using electron heating with the conductivity profiles characteristic of L-mode. Both feedback control cases demonstrate the capability to have $q(0)$ follow a preprogrammed evolution at values above that obtained without the additional heating. The controller was able to recover from mismatches between the actual q value and the target value just after breakdown and maintain $q(0)$ near the preprogrammed target value during periods when the ECH power was not saturated at the minimum or maximum.

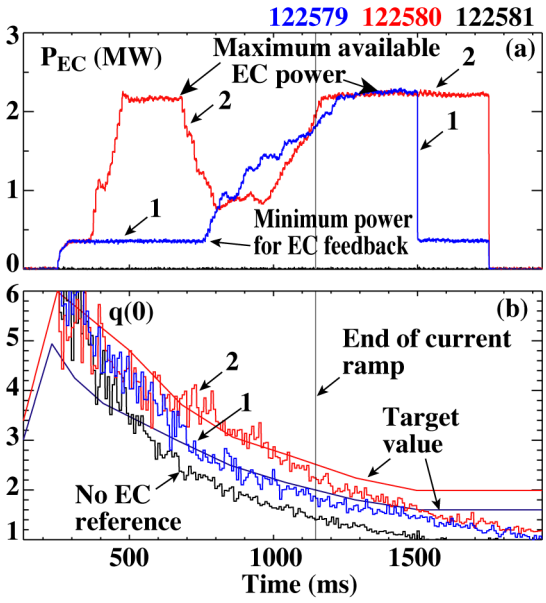

FIG. 3. Two cases of closed loop feedback control of the on-axis q in L-mode discharges using ECH at $\rho \approx 0.4$ as the actuator plus a case with no ECH or feedback control. (a) The gyrotron power. (b) A comparison of the feedback target values (smooth curves) with the real time calculation of $q(0)$. The period of active feedback ends at 1500 ms in Case 1, 1750 ms in Case 2.

The value of q_{min} has been controlled at relatively high values and for long duration using neutral beam heating in H-mode discharges. This is illustrated for two cases in Fig. 4(a) where the measured and target values of q_{min} are compared. Here, because of the increased actuator power that is available using neutral beams, the actual values of q_{min} were maintained close to the programmed levels for almost 1 s after the end of the plasma current ramp-up. The duration of the feedback control in this case was limited only by the available pulse length of the neutral beam that is required for the MSE diagnostic.

A controller utilizing only proportional gain and a controller combining proportional and integral gain (PI) have both been tested. A controller designed from a model of the poloidal flux diffusion is also being developed [13]. In the proportional gain controller [Figs. 3 and 4], the requested actuator power is equal to a preprogrammed feed-forward value plus the error in q times the gain [Fig. 4(c)]. In some cases, such as the case with ECH as the actuator shown in Fig. 3, the control could have been improved by using higher gain. However, with neutral beams as the actuator (Fig. 4), both ions and electrons are heated and there is particle fueling so the increase in β_N for a given increase in conductivity is larger than with ECH. High proportional gain could lead to excursions to unstable values of β_N. In addition, if the sampling interval for the q profile is increased to 50 ms (because the MSE beam is modulated at a low duty cycle rather than running continuously), the proportional gain controller has been observed to become unstable and the controlled q value oscillates. The PI controller, in which a value proportional to the time integral of the error in q is added to the actuator power requested by the proportional gain controller, allows operation with reduced proportional gain. The PI controller has operated successfully with the increased q profile measurement interval and can be used to limit the excursions in β_N.

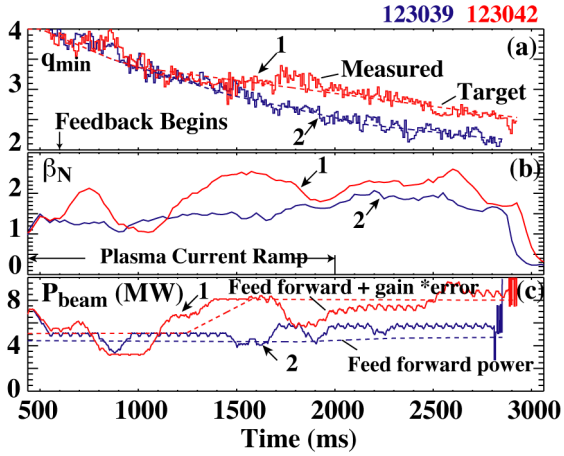

FIG. 4. Two examples of closed loop control of the minimum q value in H-mode discharges using neutral beam heating as the actuator. (a) A comparison of the feedback target values (dashed curves) with the real time calculation of q_{min}. (b) β_N. (c) A comparison of the preprogrammed feed forward neutral beam power (dashed curves) with the power actually used for feedback control. The period of feedback on q_{min} ends at 3000 ms.

5. Transport Code Simulations of Experimental Results

Comparisons of experimental measurements and transport code predictions of the time evolution of the tokamak equilibrium are used to gain a quantitative understanding of the evolution of the inductive and noninductive components of the plasma current and to validate the codes for use in testing of feedback control algorithms. Given an initial experimental equilibrium, measured density and temperature profiles as a function of time, the plasma boundary shape, and theoretical models for bootstrap current, beam-driven current and conductivity, the transport code is used to predict the time evolution of the plasma current profile. Code predictions of particular interest are q, toroidal electric field (E), and the total current density (J) and its inductive (J_{ohm}) and noninductive (J_{NI}) components. Several transport codes have been compared: ONETWO, TRANSP, CRONOS and Corsica. The codes all give similar results. Properties of the experimental equilibria are obtained from fits to magnetic and motional Stark effect diagnostic measurements using the EFIT equilibrium reconstruction code [12]. The experimental value of E is obtained [14] from the time derivative of the poloidal flux and $J_{ohm} = \sigma E$, where σ is calculated using the measured density and temperature profiles and the method of Sauter [4,5].

In L-mode discharges, such as those shown in Fig. 2(a-d), there is reasonable agreement obtained between the transport codes and experiment (Fig. 5). When the measured electron temperature and effective charge (Z_{eff}) profiles are used in the simulation, the predicted q values decrease slightly faster than what was measured [Fig. 5(c)]. If the electron temperature is increased by 20% or Z_{eff} is set to 1.0, the difference between prediction and experiment is small. These adjustments in T_e and Z_{eff} are larger than the uncertainties in the measurements, but could be interpreted as modeling an ≈30% uncertainty in the theoretical conductivity. Similarly, the agreement is reasonable between the time evolution of the measured and predicted values of the toroidal electric field at the discharge boundary and in the core [Fig. 5(d-e)] and measured and predicted profiles of J and E as shown in Fig. 6.

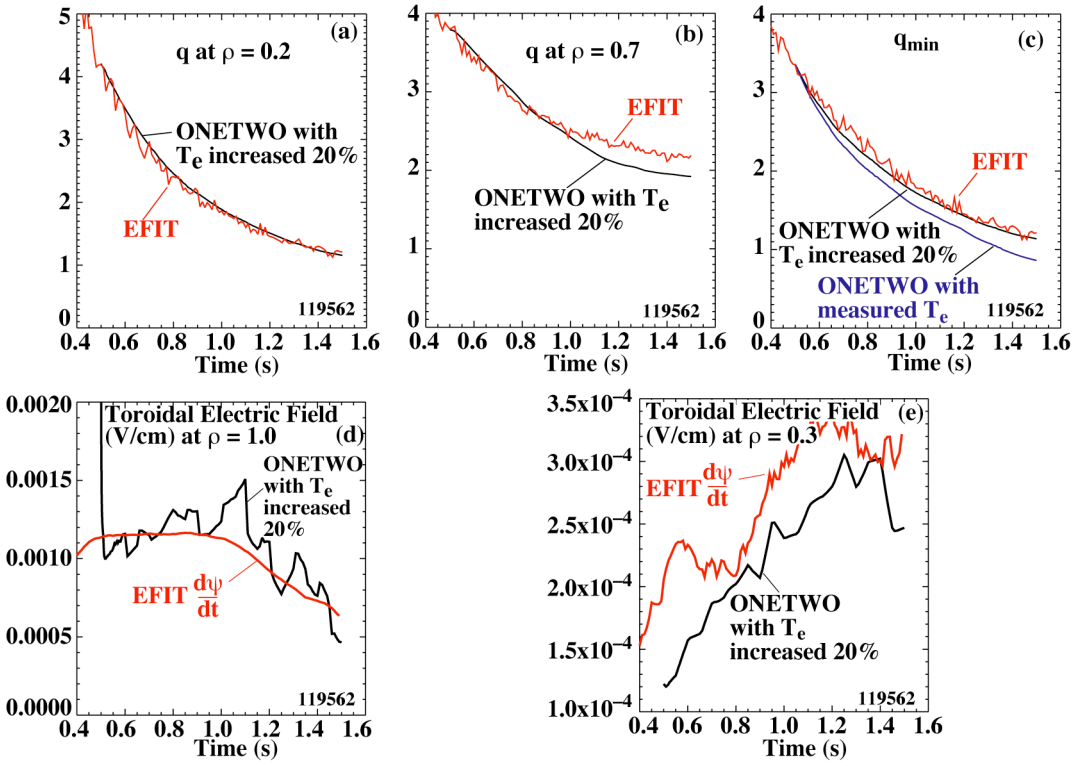

FIG. 5. For the Case 3 L-mode discharge (Fig. 2), predicted (using ONETWO) and measured values of (a-c) time evolution of q at 2 radial locations and q_{min}, (d-e) toroidal electric field at 2 radial locations.

In contrast with the relatively small differences found for L-mode discharges between the measured and predicted equilibrium properties, large differences are found for H-mode discharges between experiment and simulation using measured T_e and Z_{eff} profiles. This is illustrated by the solid lines in Fig. 7 for the Case 4 and 5 discharges in Fig. 2. In both cases, the predicted value of q_{min} (from both ONETWO and CRONOS) decreases much more quickly with time than the measured value.

Differences in the profile of J_{NI} can possibly account for the discrepancy between the codes and the experiment. Particularly in question is the profile of the neutral-beam-driven current (J_{NBCD}). A possible mechanism for altering the J_{NBCD} profile is the interaction of the beam-injected fast ions with fast-ion-driven instabilities such as the toroidal Alfvén eigenmode (TAE). There is evidence from the spectrum of measured density fluctuations that this type of instability exists in the Case 4 discharge of Fig. 2 and the discharges shown in Fig. 4. A test

was made using the CRONOS code by specifying the profile of J_{NBCD} to be a Gaussian centered at $\rho = 0.5$ with the same total neutral-beam-driven current as predicted by the theory. The width and height of the Gaussian were chosen to obtain a good match between simulation and experiment for the discharge 123042 shown in Fig. 4. As shown by the dashed line in Fig. 7, reasonably good agreement is obtained between the predicted and measured time evolutions of q_{min} for the Case 4 discharge using the same postulated shape and location of the J_{NBCD} profile. However, in the Case 5 discharge (Fig. 2) there is little evidence for Alfvén eigenmode type activity, but there is still a significant difference between the predicted and measured time evolutions of the q profile (Fig. 7) so it isn't clear that displacement of fast ions by instabilities can be the complete explanation.

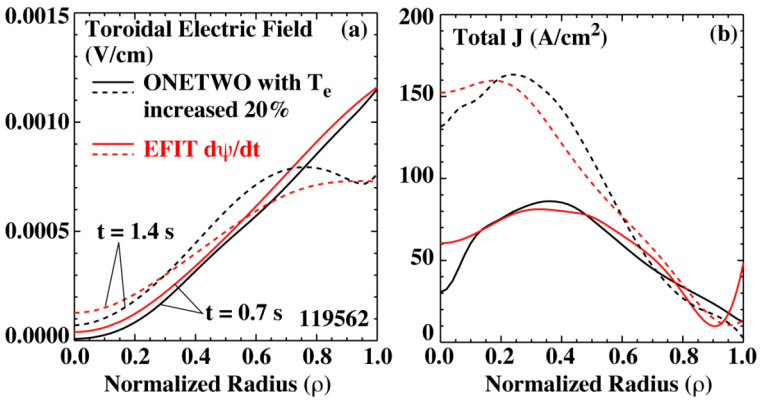

FIG. 6. Comparisons of predictions from the ONETWO transport code of (a) the toroidal electric field and (b) the total current density with the experimental values obtained from the EFIT equilibrium reconstruction code for the Case 3 L-mode discharge (Fig. 2).

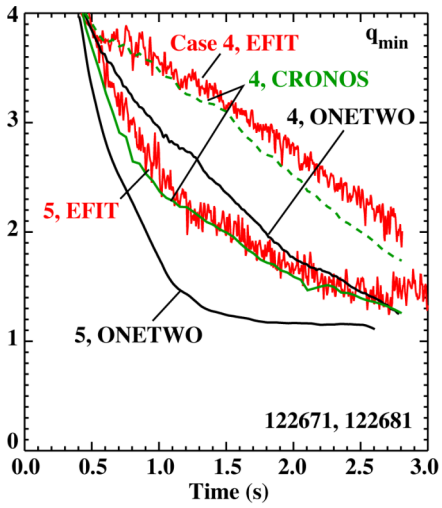

FIG. 7. Experimental and predicted time evolution of q_{min} for the Case 4 and 5 H-mode discharges shown in Fig. 2. The code predictions shown as solid lines were produced using the theoretical neutral beam driven current profile. The dashed line was produced using the postulated profile which peaks at $\rho \approx 0.5$. Black lines are predictions from ONETWO, green lines are from CRONOS.

The CRONOS code has been successfully used to model the proportional gain controller used in the experiment. In order to model the controller, the time evolutions of the plasma density, ion temperature and Z_{eff} are specified and the electron temperature profile is determined from a simple empirical model for the electron heat diffusivity based on the behavior of discharge 123042 (Fig. 4). The postulated J_{NBCD} profile described above is included. The predicted q_{min} evolution for discharge 123042 using the controller in the code to calculate the injected neutral beam power as a function of time reproduced well the experimental q_{min} evolution shown for this discharge in Fig. 4. As a more extensive test of the controller simulation, three different target waveforms for the q_{min} evolution were specified without any guide to the simulation from individual tuning of the feed-forward neutral beam power (Fig. 8). These simulations demonstrate the capability to modify the time evolution of q_{min} using feedback control of the neutral beam power, similar to the experimental results shown in Fig. 4. The simulations also show the tendency for the proportional gain controller to produce slow oscillations in the controlled q value as has been observed in the experiment.

6. Conclusion

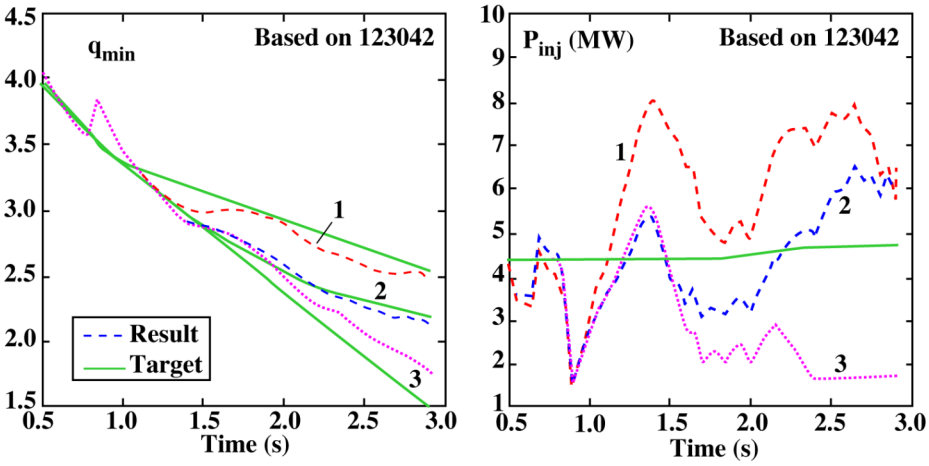

FIG. 8. Three test cases of simulating the proportional gain q_{min} controller using the CRONOS transport code. (a) Target value of q_{min} (solid lines) and predicted q_{min} value (dashed and dotted lines). (b) Feed-forward neutral beam power (solid line), the same for all 3 cases, and the required neutral beam power computed in the simulations (dashed and dotted lines).

In summary, to improve reproducibility of AT discharges in DIII-D and to facili-tate the optimization of the target q profile for the high β phase of the discharge, feedback control of the evolution of $q(0)$ and q_{min} during the initial portion of the discharge is being developed. Changes in the conductivity through electron heating are used to modify the rate of relaxation of the current profile. The q profile is obtained in real time from a complete equilibrium reconstruction using data from the MSE diagnostic. In L-mode and H-mode discharges, feedback control of q is effective with the appropriate choice of either off-axis ECH or neutral beam heating as the actuator. Comparisons of experimental measurements and transport code predictions of the time evolution of the current profile are used to validate transport codes for use in testing of real time feedback control algorithms. In some cases, the modeled noninductive current must be located farther from the axis than is predicted by theory in order to obtain agreement between the simulations and the experiment.

This work was supported in part by the U.S. Department of Energy under DE-FC02-04ER54698, W-7405-ENG-48, DE-FG03-01ER54615, DE-AC05-00OR22725, DE-FG02-92ER54141, and DE-AC05-76OR00033.

References

[1] TAYLOR, T.S., Plasma Phys. Control. Fusion **39** (1997) B47.
[2] MURAKAMI, M., *et al.*, Phys. Plasmas **13** (2006) 056106.
[3] FERRON, J.R., *et al.*, Nucl. Fusion **46** (2006) L13.
[4] SAUTER, O., *et al.*, Phys. Plasmas **6** (1999) 2834.
[5] SAUTER, O., *et al.*, Phys. Plasmas **9** (2002) 5140.
[6] MIKKELSEN, D.R., *et al.*, Phys. Fluids B **1** (1989) 333.
[7] BATHA, S.H., *et al.*, Controlled Fusion and Plasma Physics **19C**, Vol. II (Petit Lancy, European Physical Society 1995) p. 113.
[8] RICE, B.W., *et al.*, Plasma Phys. Control. Fusion **38** (1996) 869.
[9] FERRON, J.R., *et al.*, Proc. of the 29th EPS Conf. on Plasma Physics and Controlled Fusion, Montreux, 2002, ECA Vol. 26B, P1.060.
[10] FERRON, J.R., *et al.*, Nucl. Fusion **38** (1998) 1055.
[11] RICE, B.W., *et al.*, Phys. Rev. Lett. **79** (1997) 2694.
[12] LAO, L.L., *et al.*, Fusion Sci. and Technol. **48** (2005) 968.
[13] OU, Y., *et al.*, "Model-based Current Profile Control at DIII-D," presented at the 24th Symposium on Fusion Technology, Warsaw (2006) and to be published in Fusion Eng. and Design.
[14] FOREST, C.B., *et al.*, Phys. Rev. Lett. **73** (1994) 2444.